NATIONAL INSTITUTE OF POLAR RESEARCH

ANTARCTIC GEOLOGICAL MAP SERIES
SHEET 19 TENMONDAI ROCK

Explanatory Text of Geological Map of Tenmondai Rock, Antarctica

Kazuyuki SHIRAISHI, Yoshikuni HIROI, Kiichi MORIWAKI,
Kiyotaka SASAKI and Hitoshi ONUKI

NATIONAL INSTITUTE OF POLAR RESEARCH
TOKYO, MARCH 1985

National Institute of Polar Research
9–10, Kaga 1-chome, Itabashi-ku
Tokyo 173, Japan

Explanatory Text of Geological Map of Tenmondai Rock, Antarctica

Kazuyuki SHIRAISHI[1], Yoshikuni HIROI[2], Kiichi MORIWAKI[1], Kiyotaka SASAKI[3] and Hitoshi ONUKI[4]

1. Introduction

The Tenmondai Rock is a small ice-free area located at 68°24′ S in latitude and 41°45′ E in longitude on the Prince Olav Coast. The bedrock is exposed for about 3 km along the coastal line and about 1 km in width. The geological survey of the area was begun by K. SHIRAISHI of the 21st Japanese Antarctic Research Expedition (JARE-21) in September 1980, and completed by Y. HIROI and K. SASAKI of JARE-22 and K. SHIRAISHI in January 1981. The geomorphological survey was done by K. MORIWAKI of JARE-22 and a geodetic survey was conducted by the Geographical Survey Institute at the same time. The Tenmondai Rock appears in the topographic maps "Naga-iwa Rock" and "Gobanme Rock" on a scale of 1:25000 which were published in March 1982. An orthophotomap of about 1:10000 in scale was prepared for the field survey. Since the rock is too small to describe the results of the survey in detail, the geological maps of the two different scales (1:25000 and about 1:10000) are shown in this issue.

2. Geomorphology

The Tenmondai Rock is bounded by the Higasi-naga-iwa Glacier on the west. To the east several small rock exposures (Narabi Rocks), each of which is several hundred meters wide, are scattered along the coast.

The ice-free area shows fairly smooth topography below the height of 100 m above sea level, slopes down to the sea, and terminates with steep slopes. There is no beach deposit even on the seashore. NW-SE and NE-SW relief features develop in the area but this relief is not striking. Their trend reflects the strike of foliation and the joint system of gneissic basement rocks. A bank of shear moraine lies on the ice sheet close to the upper margin of the ice-free bedrock area. Boulders of various sizes occur as scattered ground moraines on the bedrock. Honeycomb weathering is found on the bedrock and boulders in and on ridges and coastal part. Nevertheless, many glacial striae remain in the whole area. Glacial striae are of uniform direction

1) National Institute of Polar Research, 9–10, Kaga 1-chome, Itabashi-ku, Tokyo 173.
2) Department of Earth Sciences, Faculty of Science, Chiba University, 1–33, Yayoi-cho, Chiba 260.
3) Institute of Mineralogy, Petrology and Economic Geology, Faculty of Science, Tohoku University, Aramaki Aoba, Sendai 980.
4) Department of Earth Sciences, Faculty of Science, Hirosaki University, 3, Bunkyo-cho, Hirosaki 036.

of NW-SE, crossing perpendicularly to the coastal line. Periglacial phenomena such as patterned ground and block fields are not developed well in this area.

3. Geology

3.1. General

The Tenmondai Rock is underlain by well-layered gneisses, migmatitic rocks, granite and pegmatite. Among the metamorphic rocks biotite-hornblende and hornblende-biotite gneisses are predominant, and lesser amounts of garnet-biotite gneiss and amphibolite are intercalated. Concordant sheets of pink gneissose granite occur locally. Reddish brown granite and pegmatite intrude widely along the fracture system of the well-layered and migmatitic rocks.

Extensive migmatization extends from the central to the western part of the bedrock exposure and is the most characteristic feature of the area. The migmatitic rocks show dome structures, the core of one of which is a relatively homogeneous, leucocratic, and massive rock of granodioritic composition. In addition to the dome structure of the migmatitic rocks, conspicuous tight synform and antiform structures are observed at Torihara Heights and Dome Rock, respectively, in the well-layered gneiss region (Plate 1b and 2). Small-scale undulations are seen throughout the bedrock exposure. Therefore, the total thickness of the well-layered and migmatitic rocks may be no more than several hundreds meters as inferred from the geologic profile.

Aluminous garnet-biotite gneiss usually contains both kyanite and sillimanite (HIROI *et al.*, 1983). As will be described later, kyanite always occurs as inclusions in garnet and plagioclase, suggesting that it is a metastable relic formed at an early stage of prograde metamorphism of the kyanite-sillimanite type. Moreover, andalusite rarely occurs in the kyanite-sillimanite-bearing gneisses which are cut extensively by the reddish brown granite and pegmatite (HIROI *et al.*, 1983). The field evidence and the mode of occurrence of andalusite when seen in thin section under the microscope suggest that andalusite was formed by the thermal metamorphism of the reddish brown granite and pegmatite under conditions differing from the earlier regional metamorphism.

Orthopyroxene is the diagnostic mineral of the granulite facies and occurs first in this bedrock exposure in the progressive metamorphic sequence from northeast to southwest along the Prince Olav Coast (SHIRAISHI *et al.*, 1984). However, it is very rare in occurrence in this bedrock exposure.

The basement rocks are classified into the following types based on the mode of occurrence and petrographic characteristics.

1. Garnet-biotite gneiss (Ggb)
    - 1.1. Garnet-biotite gneiss
    - 1.2. Gedrite-garnet-biotite gneiss
    - 1.3. Kyanite-bearing sillimanite-garnet-biotite gneiss
    - 1.4. Andalusite-kyanite-bearing sillimanite-garnet-biotite gneiss
2. Biotite-hornblende gneiss and hornblende-biotite gneiss (Gbh, Mbh)
3. Amphibolite (Am)
    - 3.1. Orthopyroxene amphibolite

Table 1. Chemical analyses of rocks from the Tenmondai Rock.

Sp. No.	1	2	3	4	5	6	7	8	9	10	11
SiO_2	40.06	41.09	41.17	47.81	48.23	49.95	59.67	69.76	70.49	73.07	75.78
TiO_2	2.40	0.65	1.70	1.99	1.43	1.53	0.80	0.50	0.35	0.31	0.24
Al_2O_3	15.18	20.15	17.02	17.23	18.20	15.77	15.93	13.04	14.66	13.09	11.46
Fe_2O_3	3.95	3.76	4.36	3.41	3.36	3.82	3.45	4.31	1.49	1.83	0.54
FeO	11.76	6.81	10.89	7.42	6.69	9.21	4.19	3.11	3.68	2.27	2.62
MnO	0.10	0.18	0.18	0.27	0.25	0.16	0.19	0.21	0.10	0.13	0.20
MgO	9.12	9.10	6.54	4.95	5.87	4.84	3.06	1.81	2.34	1.90	2.29
CaO	11.60	14.56	14.18	10.55	8.95	9.26	7.33	1.58	0.77	0.73	1.48
Na_2O	2.01	1.48	1.34	3.22	3.30	2.82	3.78	2.48	4.51	4.61	3.26
K_2O	1.52	0.39	0.36	1.20	1.07	0.78	0.79	1.75	0.61	0.96	1.87
H_2O (+)	1.59	1.75	1.29	1.40	2.04	1.35	0.71	0.88	0.84	0.79	0.68
H_2O (−)	0.08	0.04	0.10	0.07	0.02	0.10	0.05	0.11	0.16	0.23	0.07
P_2O_5	0.38	0.05	0.60	0.20	0.12	0.26	0.29	0.05	0.06	0.05	0.03
ZnO (ppm)								102			
Total	99.75	100.01	99.73	99.72	99.53	99.85	100.24	99.59	100.06	99.97	100.52
Q	—	—	—	—	—	2.48	15.67	41.91	34.62	37.24	41.18
C	—	—	—	—	—	—	—	4.31	5.32	3.26	1.45
Or	6.11	—	2.13	7.09	6.32	4.61	4.67	10.34	3.60	5.67	11.05
Ab	—	—	7.37	25.73	27.92	23.86	31.99	20.99	38.16	39.01	27.59
An	27.91	47.19	39.36	29.02	31.69	28.07	24.17	7.51	3.43	3.29	7.15
Lc	2.25	1.81	—	—	—	—	—	—	—	—	—
Ne	9.21	6.78	2.15	0.82	—	—	—	—	—	—	—
Di wo	11.34	10.30	11.30	9.19	4.98	6.75	4.30	—	—	—	—
Di en	6.59	6.82	5.92	5.31	3.08	3.38	2.68	—	—	—	—
Di fs	4.22	2.73	5.06	3.45	1.61	3.23	1.36	—	—	—	—
Hy en	—	—	—	—	3.06	8.68	4.94	4.51	5.83	4.73	5.70
Hy fs	—	—	—	—	1.59	8.30	2.51	1.72	5.13	2.39	4.34
Ol fo	11.30	11.10	7.27	4.92	5.94	—	—	—	—	—	—
Ol fa	7.98	4.90	6.85	3.53	3.41	—	—	—	—	—	—
Mt	5.73	4.73	6.32	4.94	4.87	5.54	5.00	6.25	2.16	2.65	0.78
Il	4.56	1.23	3.22	3.78	2.72	2.91	1.52	0.95	0.66	0.59	0.46
Ap	0.88	0.12	1.39	0.46	0.28	0.60	0.67	0.12	0.14	0.12	0.07
Analyst	A	A	A	A	A	A	B	C	A	A	B

No.		
1.	81012406	Biotite amphibolite
2.	80T15	Scapolite-bearing clinopyroxene amphibolite
3.	81012301	Scapolite-bearing clinopyroxene amphibolite
4.	81T136	Clinopyroxene-quartz-bearing biotite amphibolite
5.	81T126	Clinopyroxene-bearing biotite amphibolite
6.	81012509A	Biotite-quartz-bearing clinopyroxene amphibolite
7.	80T21	Biotite-hornblende gneiss
8.	81012409	Andalusite-kyanite-bearing sillimanite-garnet-biotite gneiss
9.	81012514A	Gedrite-garnet-biotite gneiss
10.	81012514B	Spinel-bearing garnet-biotite gneiss
11.	80T32	Garnet-biotite gneiss

Analyst; A: H. ONUKI and M. TEZUKA, B: Japan Chemical Analysis Center, C: T. HIRANO.

3.2. Biotite amphibolite
3.3. Clinopyroxene amphibolite
4. Granodioritic migmatite (Mg)
5. Pink gneissose granite (Gg)
6. Reddish brown granite and pegmatite (Gr, P)

Representative bulk chemical compositions of the rocks are presented in Table 1.

3.2. Geology and petrography

3.2.1. Garnet-biotite gneiss

1) Garnet-biotite gneiss: Garnet-biotite gneiss occurs mainly in the eastern and western parts of the bedrock exposure as a well-layered gneiss in conjunction with other gneisses. It also occurs as thin layers up to several meters thick in the central part where migmatitic rocks predominate. The garnet-biotite gneiss typically shows a banded structure of alternating thin layers up to 2 cm thick, rich in mafic minerals and rich in felsic minerals. The constituent minerals of the common Al-poor garnet-biotite gneiss are garnet, biotite, plagioclase, quartz, apatite, zircon and opaque minerals with or without K-feldspar. Muscovite, chlorite, and calcite are also present in small amounts as secondary minerals. Garnet usually occurs as porphyroblasts up to 1 cm in diameter, and occasionally shows a "snow ball" texture. Garnet-biotite gneiss includes some varieties as follows.

2) Gedrite-garnet-biotite gneiss: This rock occurs only in the central part of the exposure together with gedrite-free garnet-biotite gneiss. It is composed of gedrite, garnet, biotite, plagioclase, quartz, magnetite, apatite, zircon, and pyrite. Trace amount of green spinel is also present in close association with magnetite. Gedrite is usually replaced by brown "pinite" partially.

3) Kyanite-bearing sillimanite-garnet-biotite gneiss: This rock is developed mainly in the eastern part of the bedrock exposure. Constituent minerals are spinel, kyanite, sillimanite, garnet, biotite, plagioclase, K-feldspar, quartz, apatite, zircon, and opaque minerals. Secondary muscovite, chlorite, and calcite are also present in small amounts. Spinel and kyanite always occur as inclusions in garnet and plagioclase, and are never in direct contact with quartz (Plate 8b). On the other hand, sillimanite is in contact with most minerals present. Therefore, kyanite is a metastable relic formed at an early stage of prograde recrystallization of the rock. The close association spinel+kyanite+garnet is the dehydrated equivalent of staurolite, which is known to occur in the eastern part of the Prince Olav Coast (HIROI *et al.*, 1983). This suggests that staurolite broke down in the kyanite stability field during the prograde recrystallization of the rock.

4) Andalusite-kyanite-bearing sillimanite-garnet-biotite gneiss: This rock occurs in the eastern part of the bedrock exposure, and belongs to the same stratum of kyanite-bearing sillimanite-garnet-biotite gneiss mentioned above. The significant field evidence is that the rock is cut by the reddish brown granite and pegmatite. Under the microscope, andalusite occurs in a small amount, being accompanied by muscovite. It occasionally includes sillimanite (Plate 8c). Therefore, it is safely concluded that andalusite was formed by the thermal metamorphism of the reddish brown granite and pegmatite.

3.2.2. Biotite-hornblende gneiss and hornblende-biotite gneiss

These gneisses predominate in this bedrock exposure. Although biotite-hornblende gneiss is more abundant than hornblende-biotite gneiss, these rocks are closely intercalated. Both show a well-layered structure with other rocks and also a banded structure of alternating salic and mafic layers up to a few cm in thickness. These structures are distinct in the eastern and western parts of the area, but on the other hand, they are often ambiguous in the central part where extensive migmatization occurs. Here various migmatitic structures such as surreitic, schollen, stromatic, schlieren and nebulitic are observed (Plates 3–6). The leucosome of the migmatitic rocks is generally granodioritic in composition. Constituent minerals are biotite, hornblende, plagioclase, K-feldspar, quartz, apatite, zircon, and opaque minerals. Secondary tremolite, chlorite, muscovite, and calcite are also present in small amounts.

3.2.3. Amphibolite

Amphibolite occurs as concordant thin layers up to a few tens of meters thick with other well-layered gneisses and as boundinages, pods, and agmatitic blocks in the migmatitic rocks.

1) Orthopyroxene amphibolite: This rock occurs as a paleosome within migmatitic biotite-hornblende gneiss. It is recognized with the naked eye by brown orthopyroxene associated with dark green hornblende, black biotite, and pale greenish brown plagioclase. Under the microscope, orthopyroxene occurs as anhedral poikiloblastic and granoblastic grains, and sometimes includes hornblende (Plate 9b). It shows very strong pleochroism. The rock is quartz-free and contains as accessory minerals ilmenite, magnetite, apatite, zircon, and pyrite. Representative microprobe analyses of the constituent minerals are listed in Table 3 of SHIRAISHI *et al.* (1984).

2) Biotite amphibolite: This is the most common type of amphibolite in the present area, and is a medium-grained rock with granoblastic to lepidoblastic textures. The usual constituent minerals are hornblende, biotite, plagioclase with or without K-feldspar and quartz. Garnet is sometimes found (Plate 10a). Accessory minerals are sphene, apatite, zircon, and opaque minerals. Secondary chlorite, tremolite, and magnesite are also present in small amounts. Plagioclase in quartz-free rocks is often zoned chemically.

3) Clinopyroxene amphibolite: This rock is melanocratic and fine- to medium-grained. The constituent minerals are clinopyroxene, hornblende, plagioclase, apatite, zircon, and opaque minerals with or without K-feldspar, quartz, scapolite and biotite. Plagioclase in quartz-free rocks is often zoned chemically. Scapolite occurs only in rocks free from quartz. In some cases, the rock is extremely poor in Al and tremolite and phlogopitic biotite occur instead of common hornblende and biotite (Plate 10b).

3.2.4. Granodioritic migmatite

A relatively homogeneous, leucocratic, and medium- to coarse-grained rock of granodioritic to tonalitic composition occurs at Aka-iwa Rock in the central part of the bedrock exposure. It is located at the core of the dome structure of the migmatitic rocks. Basic schlieren consisting of hornblende and biotite gives a foliated structure to the rock. Xenolithic blocks of basic to ultrabasic composition are included in the marginal part of the granodioritic migmatite. This rock gradually changes to migmatitic biotite-hornblende and hornblende-biotite gneisses. The constituent minerals are hornblende, biotite, plagioclase, K-feldspar, quartz, apatite, zircon, and opaque minerals. Plagioclase is often antiperthitic. In some cases, tremolitic amphibole and phlogopitic biotite occur instead of common hornblende and biotite. Muscovite and chlorite of secondary origin are commonly present in small amounts.

3.2.5. Pink gneissose granite

Pink gneissose granite occurs locally both in the well-layered gneisses and in the migmatitic rocks. It is a medium- to coarse-grained rock. The pink color is due to the presence of abundant K-feldspar (microcline). It consists of biotite, hornblende, K-feldspar, plagioclase, quartz, apatite, zircon, and opaque minerals. Secondary muscovite, chlorite, and calcite are common.

3.2.6. Reddish brown granite and pegmatite

It is also a characteristic feature of this bedrock exposure that abundant reddish brown granite and pegmatite dikes intrude the well-layered and migmatitic rocks. The thickness of the dikes ranges from a few centimeters to a few tens of meters. Small stocks and pools of the granite are seen at the southern cliff of Dome Rock (Plate 2). The dikes often intrude along one of the fractures of the well-layered and migmatitic rocks trending NE-SW, but it is not uncommon that networks of the dikes cut the country rocks into pieces. Both the granite and pegmatite are composed of K-feldspar, plagioclase, and quartz with a small amount of biotite. Accessory magnetite and ilmenite and secondary muscovite and chlorite are also present. In some cases, magnetite and ilmenite accompanied by small amounts of biotite, muscovite, corundum, plagioclase, zircon and apatite make up a lens-shaped body up to 40 cm in thickness (Plates 6b and 10c).

3.3. Geologic structure

Within the migmatitic rock area, the trend of foliation is variable, but a definite dome structure is observed at Aka-iwa Rock. On the other hand, the foliation of the well-layered gneisses consistently trends NW-SE. Dips are variable, but those of 40–85°SW are predominant.

On a macroscopic scale, a tight synform at Torihane Heights and a closed antiform at Dome Rock are conspicuous. The latter is well observed at the southern cliff of Dome Rock (Plate 2). Disharmonic folds develop at the hinge of the antiform.

Mesoscopic isoclinal to closed folds are often found in which intrafolial folds are not common. The axes of isoclinal to closed folds plung 10 to 22° SE, and their axial planes usually incline westwards.

Mineral lineations are defined by the linear arrangement of mafic minerals such as hornblende and biotite or that of prismatic mineral like sillimanite. These plunge in the same direction as the fold axes.

On the other hand, open folds with axial traces trending E-W to NE-SW are occasionally observed. The wavelength of such open folds ranges from several decimeters to a few meters. Thus the well-layered gneisses have been folded, at least, twice.

In addition, both well-layered gneisses and migmatitic rocks are sometimes folded locally near the reddish brown granite and pegmatite dikes (Plate 7a). Such a local deformational feature is clearly different from those mentioned above, and may be related to the intrusion of the granite and pegmatite.

A left-lateral fault trending NE-SW is found in the migmatitic rock area. The strike slip is not more than a few meters. The fault plane has been eroded, and there is a trench filled with gravel at the exact position of the fault.

A set of joints with trends of NE-SW and NW-SE are conspicuous throughout the bedrock exposure. Although the dips of the joints are nearly vertical, the latter trend is almost parallel to that of the foliation of the well-layered gneisses.

Acknowledgments

We would like to express our sincere thanks to Mr. T. HIRANO of Akita University for the chemical analysis of a specimen. We also greatly thank Dr. A. GRAHAM of British Museum for his kind correction of English. Thanks are extended to Mr. H. KOJIMA of National Institute of Polar Research and to Mr. Y. MOTOYOSHI of Hokkaido University for their cordial assistance to us.

References

HIROI, Y., SHIRAISHI, K., YANAI, K. and KIZAKI, K. (1983): Aluminum silicates in the Prince Olav and Sôya Coasts, East Antarctica. Mem. Natl Inst. Polar Res., Spec. Issue, **28**, 115–131.

SHIRAISHI, K., HIROI, Y. and ONUKI, H. (1984): Orthopyroxene-bearing rocks from the Tenmondai and Naga-iwa Rocks in the Prince Olav Coast, East Antarctica; First appearance of orthopyroxene in progressive metamorphic sequence. Mem. Natl Inst. Polar Res., Spec. Issue, **33**, 126–144.

(Received January 18, 1985)

a. Aerial photograph of the Tenmondai Rock. JARE Antarctic air photograph.

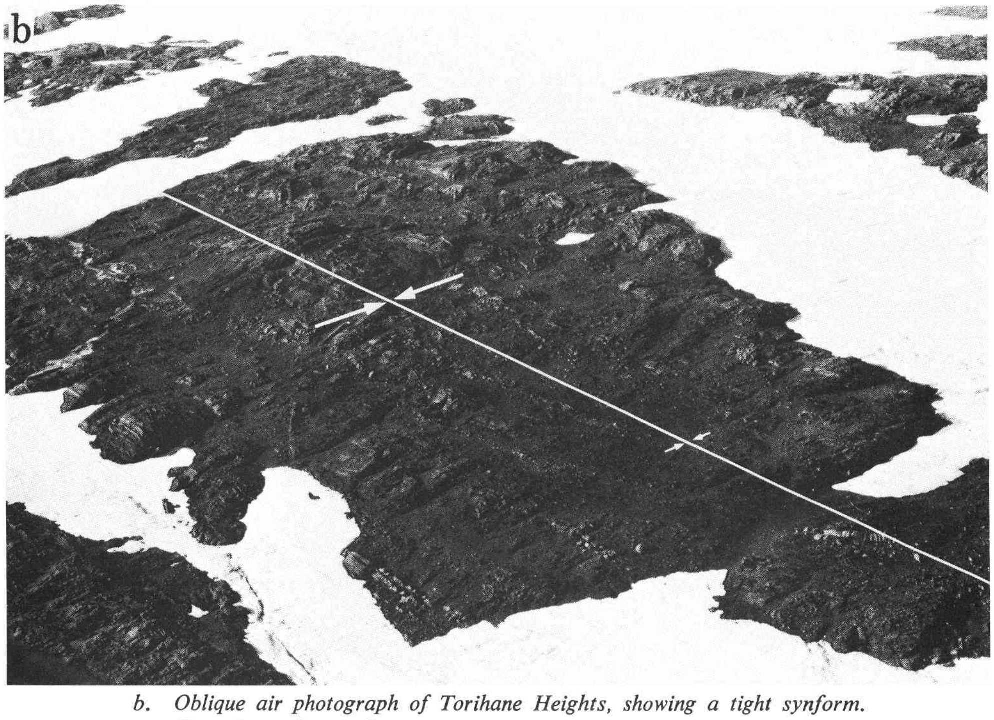

b. Oblique air photograph of Torihane Heights, showing a tight synform. View from the northeast.

Plate 2

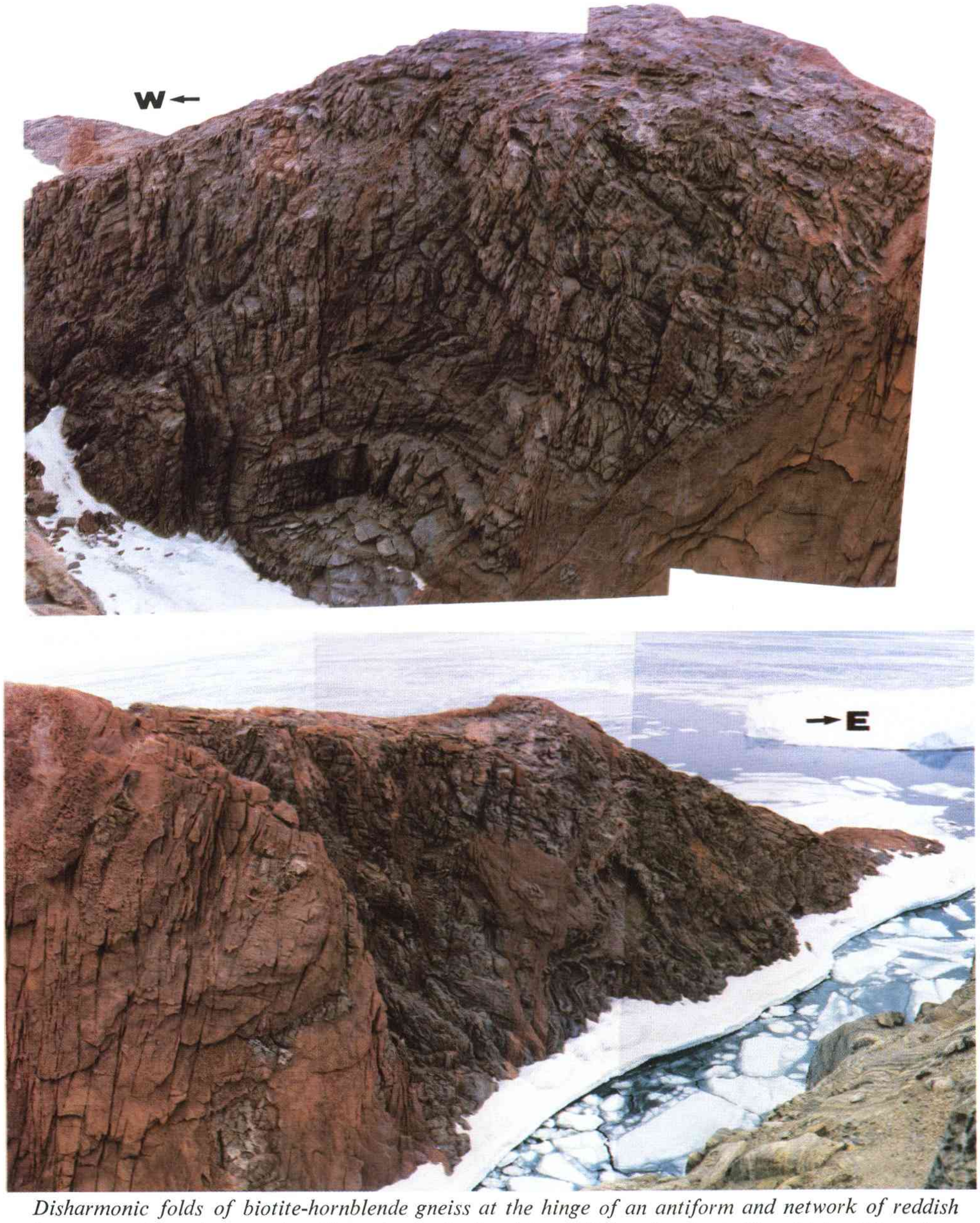

Disharmonic folds of biotite-hornblende gneiss at the hinge of an antiform and network of reddish brown granite and pegmatite dikes, Dome Rock. The cliff face is about 50 m high. View from the south.

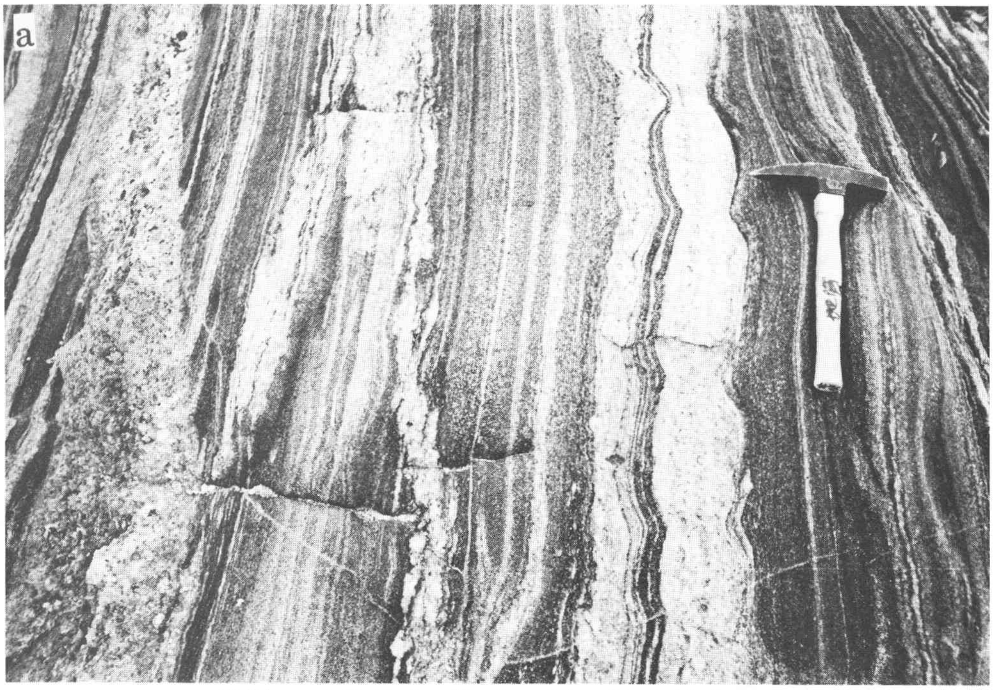

a. Well-layered biotite-hornblende and hornblende-biotite gneisses.

b. Surreitic structure of migmatitic rocks.

Plate 4

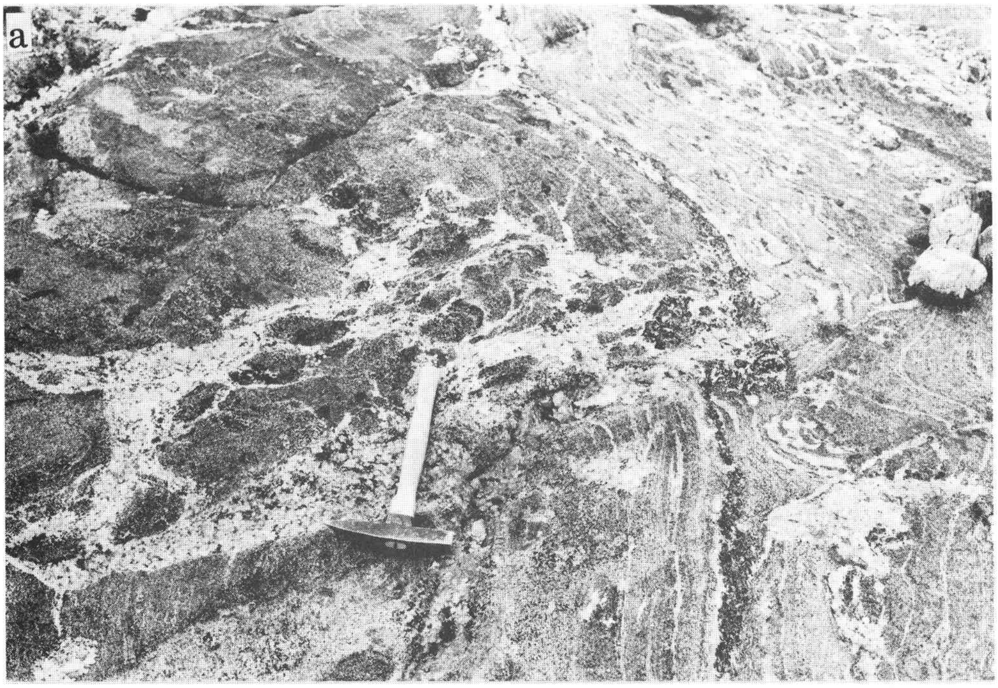

a. Schollen structure of migmatitic biotite-hornblende and hornblende-biotite gneisses.

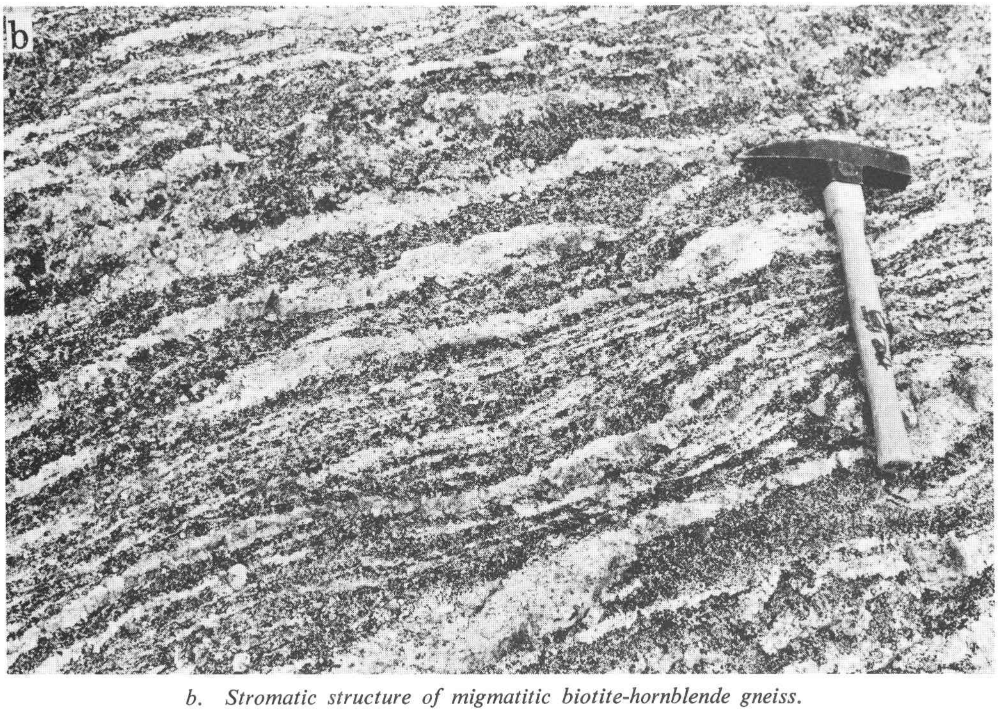

b. Stromatic structure of migmatitic biotite-hornblende gneiss.

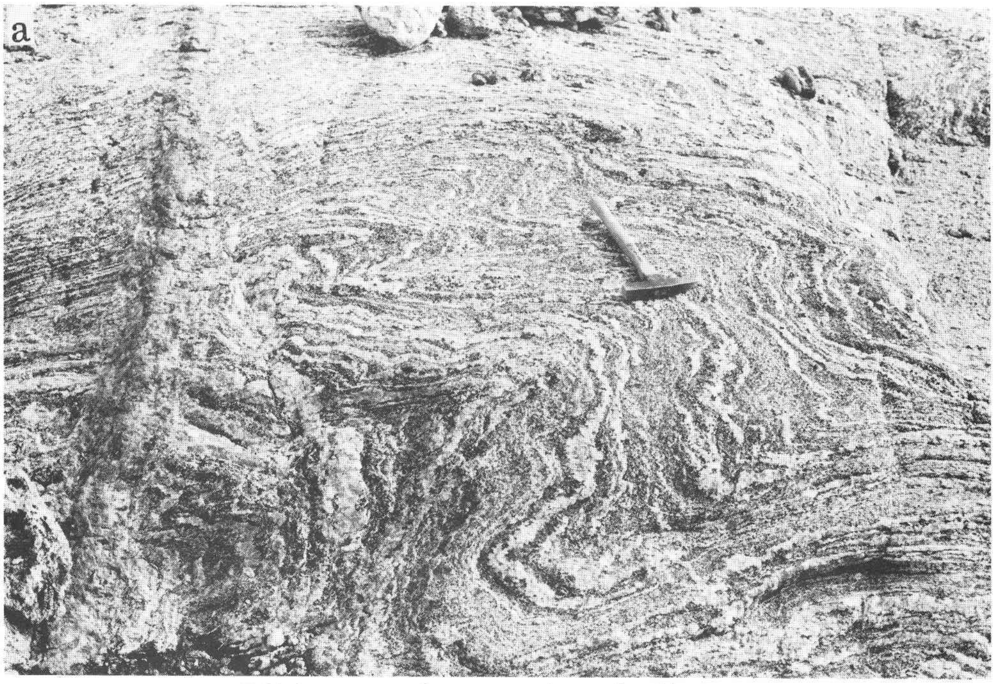

a. Folded structure of migmatitic biotite-hornblende gneiss.

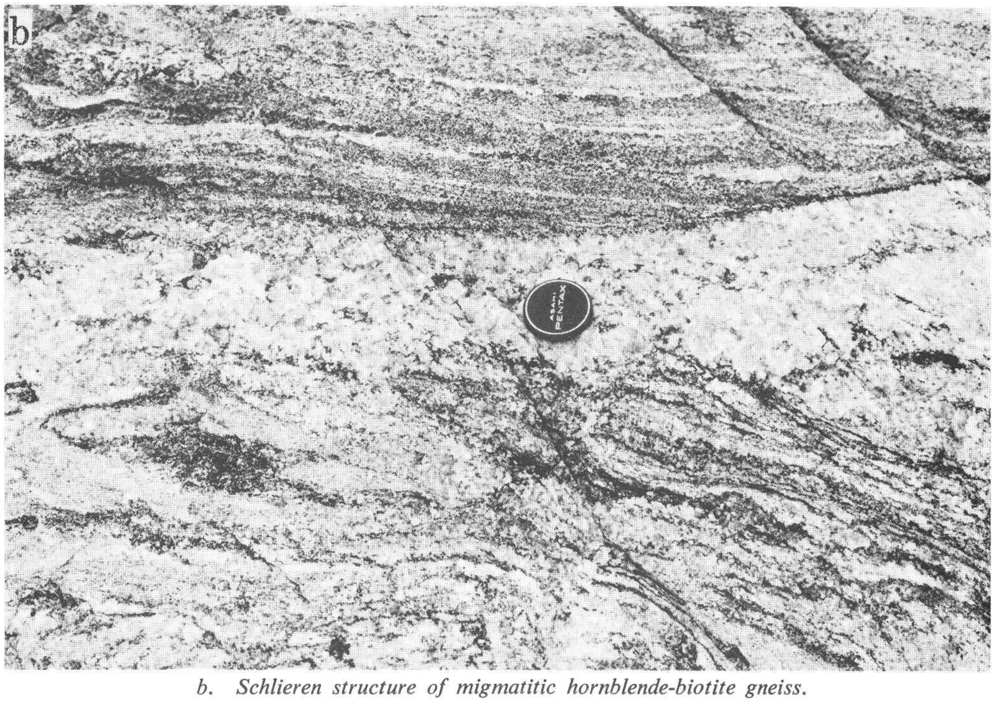

b. Schlieren structure of migmatitic hornblende-biotite gneiss.

Plate 6

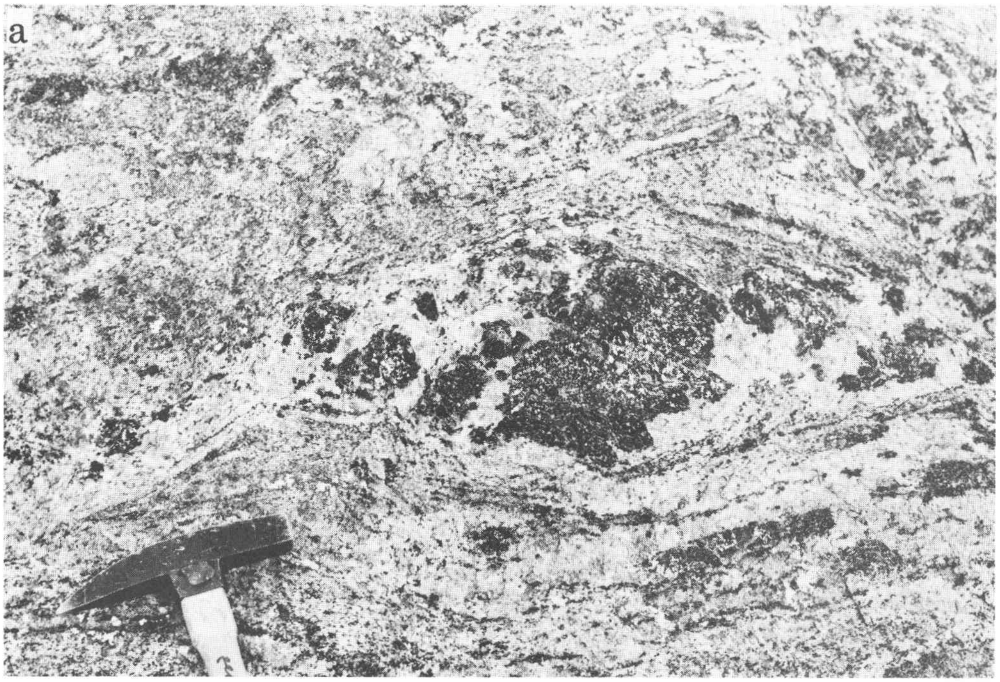

a. Nebulitic structure of migmatitic biotite-hornblende gneiss with xenolithic mafic remnants.

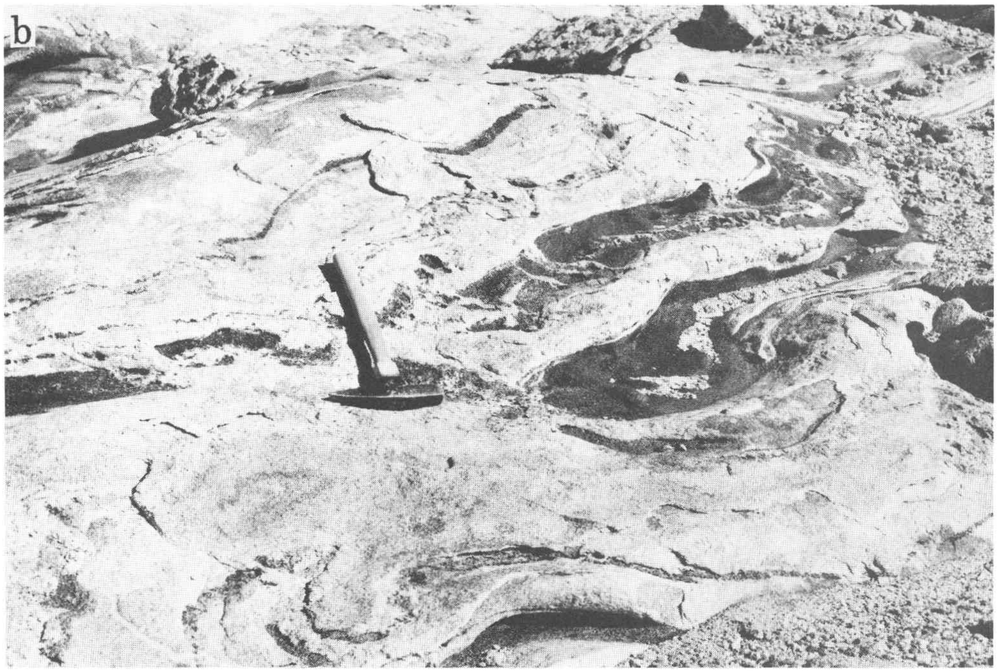

b. Homogeneous and leucocratic granodioritic rock with xenolithic mafic remnants at the core of a dome structure of migmatitic rocks, Aka-iwa Rock.

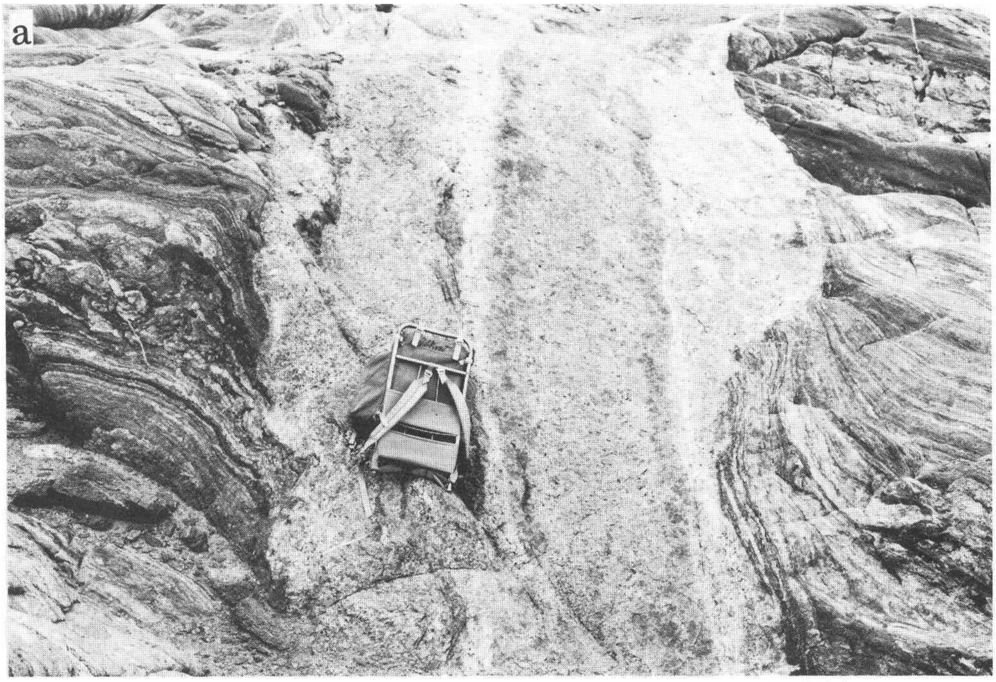

a. Composite dike of reddish brown granite and pegmatite and local folding of well-layered gneisses.

b. Ore lens composed mainly of magnetite and ilmenite in reddish brown pegmatite.

Plate 8

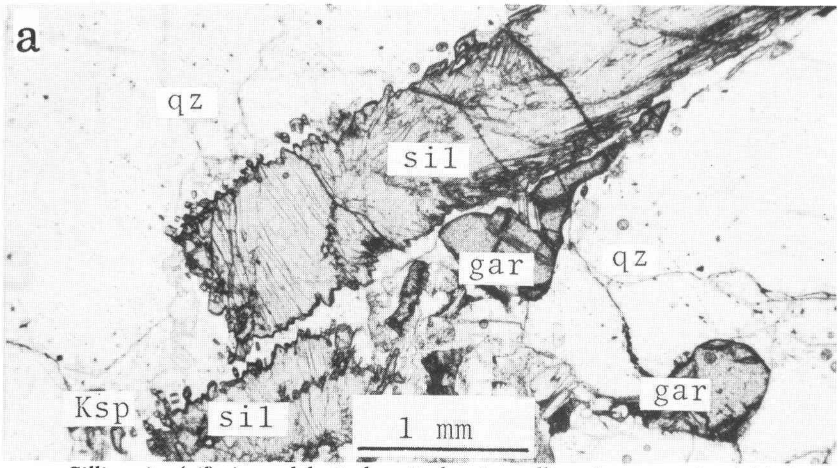

a. Sillimanite (sil) in andalusite-kyanite-bearing sillimanite-garnet (gar)-biotite gneiss (Sp. 81012409). Ksp; K-feldspar, qz; quartz.

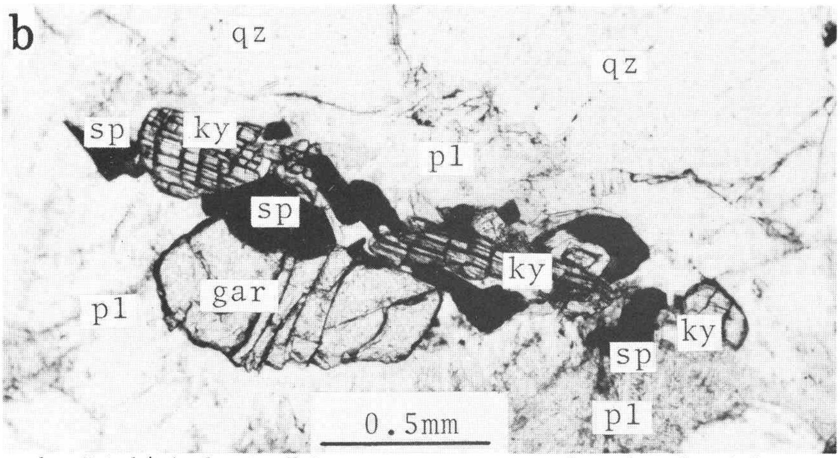

b. Spinel (sp)+kyanite (ky)+garnet association within plagioclase (pl) in andalusite-kyanite-bearing sillimanite-garnet-biotite gneiss (Sp. 81012409). Note spinel and kyanite are never in direct contact with quartz.

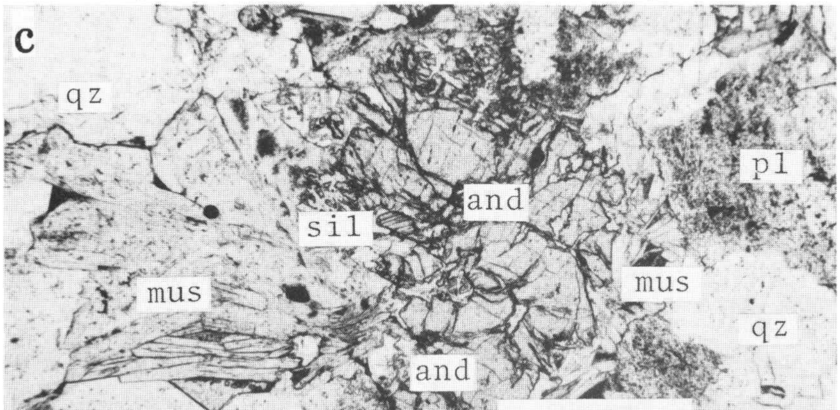

c. Andalusite (and) in andalusite-kyanite-bearing sillimanite-garnet-biotite gneiss (Sp. 81012409). Note small inclusion of sillimanite in andalusite which is in close association with muscovite (mus).

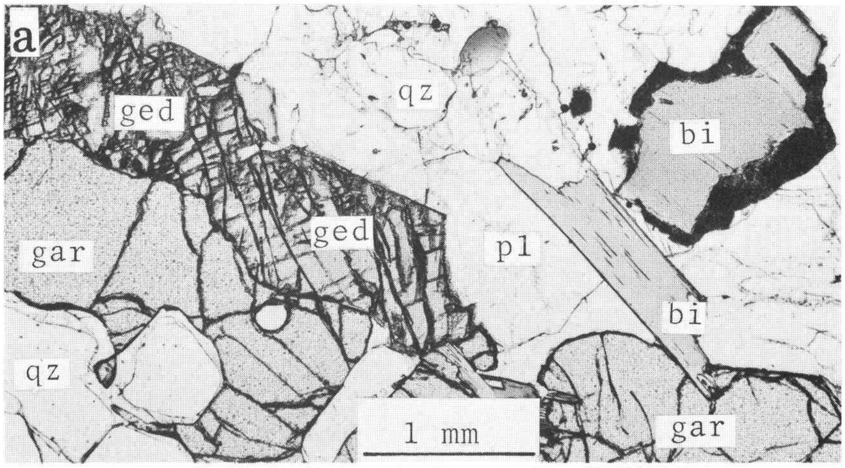

a. Gedrite (ged)-garnet-biotite gneiss (Sp. 81012514A).

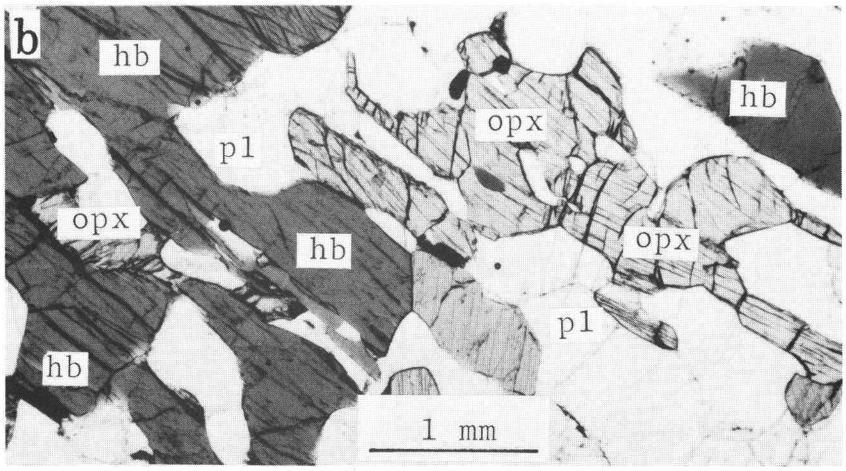

b. Orthopyroxene (opx) amphibolite (Sp. 80T10). hb; hornblende.

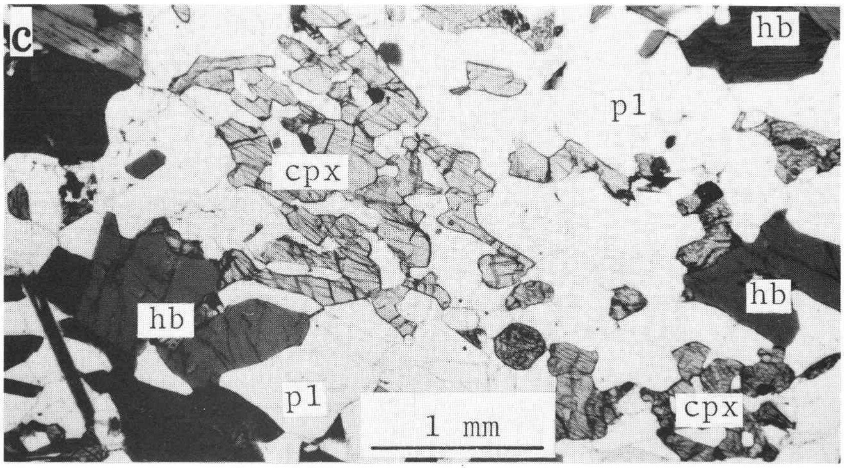

c. Clinopyroxene (cpx) amphibolite (Sp. 81012509A).

Plate 10

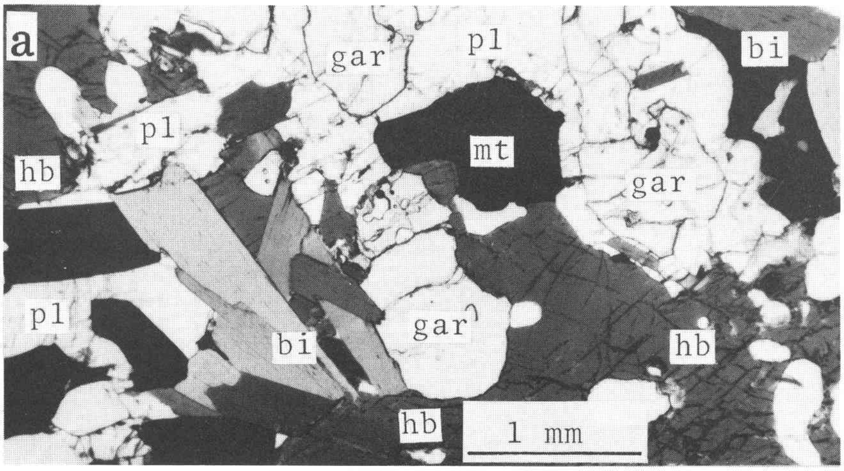

a. Garnet-bearing biotite amphibolite (Sp. 81012407). mt; magnetite.

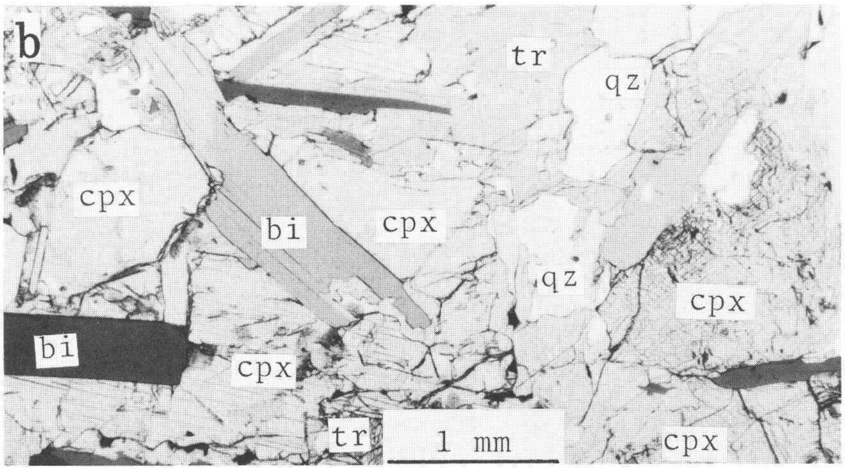

b. Clinopyroxene+tremolite (tr)+biotite+quartz association in Al-poor amphibolite (Sp. 81T124).

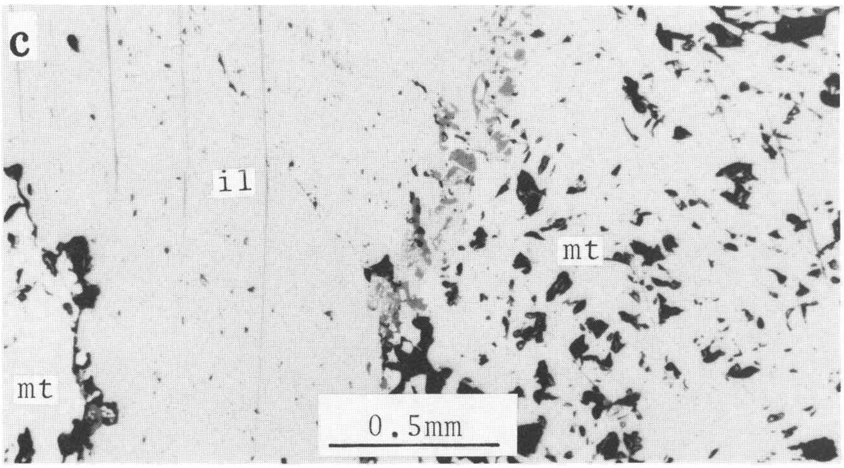

c. Magnetite and ilmenite (il) of magnetite-ilmenite lens (Sp. 81012513) in reddish brown pegmatite.

Antarctic Geological Map Series

Sheet 1	East Ongul Island	March 1974
Sheet 2	West Ongul Island	March 1974
Sheet 3	Teöya	March 1975
Sheet 4	Ongulkalven Island	March 1975
Sheet 5	Langhovde	March 1976
Sheet 6 & 7	Skarvsnes	March 1977
Sheet 8	Kjuka and Telen	March 1979
Sheet 9	Skallen	March 1976
Sheet 10	Padda Island	March 1977
Sheet 11	Cape Hinode	March 1978
Sheet 14	Sinnan Rocks	March 1983
Sheet 15	Cape Ryûgû	March 1980
Sheet 17	Niban Rock	March 1983
Sheet 18	Kasumi Rock	March 1984
Sheet 19	Tenmondai Rock	March 1985
Sheet 20	Akarui Point and Naga-iwa Rock	March 1984
Sheet 21	Cape Omega	March 1979
Sheet 22	Oku-iwa Rock	March 1981
Sheet 26	Strandnibba	March 1985
Sheet 27(1)	Mt. Fukushima, Northern Yamato Mountains	March 1978
Sheet 28	Central Yamato Mountains, Massif B and Massif C	March 1982
Sheet 29	Belgica Mountains	March 1981